

**Proceeding Series of the Brazilian Society of Computational and Applied Mathematics**

---

## 3D simulations of phase separation with a liquid crystal component

Rudimar Luiz Nós<sup>1</sup>

Departamento Acadêmico de Matemática, UTFPR, Curitiba, PR

Hector Daniel Ceniceros<sup>2</sup>

Department of Mathematics, UCSB, Santa Barbara, CA

Alexandre Megiorin Roma<sup>3</sup>

Departamento de Matemática Aplicada, USP, São Paulo, SP

**Abstract.** We present three-dimensional numerical simulations of a binary mixture with a nematic liquid crystal and flexible polymer phases using Model B, which is defined by coupling the Cahn-Hilliard equation with the de Gennes-Prost equation. The model is based on the Ginzburg-Landau free energy and the purpose of the work is to analyze in three dimensions how the orientational distortion of the director field induced by interfacial anchoring affects the morphology of the binary mixture.

**Keywords.** Cahn-Hilliard equation, Model B, Planar and homeotropic anchoring, Nematic liquid crystal.

## 1 Introduction

Binary alloys and polymer blends have been extensively studied [2] [3] and systems in which one of the components is a liquid crystal are receiving more attention [4] [5] [10] [12] [13] [18]. In this work<sup>4</sup> we simulate numerically the phase separation kinetics of a three-dimensional binary system in which one of the components is a nematic<sup>5</sup> liquid crystal and the other component is a flexible polymer with Ginzburg-Landau free energy [11] [16] [17]. The system is modeled through an order parameter or phase field  $\phi$ , which is a measure of the volume fraction of one of the components, and a director field  $\mathbf{n}$ , which quantifies the mean orientational order in the nematic liquid crystal phase [8]. This model is called Model B according to the nomenclature of Hohenberg and Halperin [9] and its dynamics are driven by energy minimization with conserved  $\phi$ . Particularly, the model that we employ differs from that considered by [19] because we keep both elastic and anchoring terms in the Cahn-Hilliard equation.

---

<sup>1</sup>rudimarnos@utfpr.edu.br

<sup>2</sup>hdc@math.ucsb.edu

<sup>3</sup>roma@ime.usp.br

<sup>4</sup>This research has been funded by Capes.

<sup>5</sup>Relating to or denoting a state of a liquid crystal in which the molecules are oriented in parallel but not arranged in well-defined planes.

This work is a 3D extension of the study by Mata, Garcia-Cervera, and Cenicerros [11]. The numerical methodology is inspired from the works [6] [7] [14] [15].

## 2 Mathematical model

Model B can be described with a phase field  $\phi$  related to the species concentration and with the director field  $\mathbf{n}$ , which is a measure of the mean molecular orientation in the nematic liquid crystal phase. The pure, bulk phases are identified with  $\phi = 1$  (red in simulations) and  $\phi = -1$  (blue in simulations) for the nematic liquid crystal and the flexible polymer component, respectively. A narrow neighborhood of the level set  $\phi = 0$  provides a diffuse interface between the two species. The equations of the mathematical model [11] [16] [17] are given by

$$\begin{aligned} \frac{\partial \phi_1}{\partial t} = & \gamma \lambda \nabla^2 \phi_2 + \\ & + \gamma \nabla^2 \left[ \frac{\lambda}{\varepsilon^2} (\phi_1^3 - \phi_1) + \frac{K}{4} \left( \nabla \mathbf{n} : (\nabla \mathbf{n})^T + \frac{(|\mathbf{n}|^2 - 1)^2}{2\delta^2} \right) + \mu_{\text{anch}} \right] + \\ & - \gamma \lambda \frac{\alpha}{\varepsilon^2} \nabla^2 \phi_1, \end{aligned} \quad (1)$$

$$\phi_2 = \frac{\alpha}{\varepsilon^2} \phi_1 - \nabla^2 \phi_1, \quad (2)$$

$$\frac{\partial \mathbf{n}}{\partial t} = \tau K \left[ \nabla \cdot \left( \frac{1 + \phi_1}{2} \nabla \mathbf{n} \right) - \frac{1 + \phi_1}{2} \frac{(|\mathbf{n}|^2 - 1) \mathbf{n}}{\delta^2} \right] - \tau \mathbf{g}, \quad (3)$$

where  $\mu_{\text{anch}}$  is given by

$$\mu_{\text{anch}} = \begin{cases} -A \nabla \cdot [(\mathbf{n} \cdot \nabla \phi_1) \mathbf{n}] & \text{(planar anchoring),} \\ -A \nabla \cdot [|\nabla \phi_1|^2 \mathbf{n} - (\mathbf{n} \cdot \nabla \phi_1) \mathbf{n}] & \text{(homeotropic anchoring),} \end{cases} \quad (4)$$

and  $\mathbf{g}$  by

$$\mathbf{g} = \begin{cases} A(\mathbf{n} \cdot \nabla \phi_1) \nabla \phi_1 & \text{(planar anchoring),} \\ A [ |\nabla \phi_1|^2 \mathbf{n} - (\mathbf{n} \cdot \nabla \phi_1) \nabla \phi_1 ] & \text{(homeotropic anchoring).} \end{cases} \quad (5)$$

In Equations (1)-(5):  $\phi_1 = \phi$ ;  $\gamma = 1$  is the constant mobility;  $\lambda$  is the mixing energy density;  $\varepsilon$  is the capillary width;  $K$  is the elastic constant for splay, twist, and bend;  $(|\mathbf{n}| - 1)^2/(2\delta^2)$  is a penalty term to approximately enforce the constraint  $|\mathbf{n}| = 1$ ;  $\tau$  is a measure of the relaxation time of the director;  $\alpha$  and  $\beta$  are numerical parameters to relax the time step stability constraint [1]; and  $A$  is the strength of the anchoring. The planar anchoring energy density favors alignment of the director tangential to the interface whereas for the homeotropic anchoring the alignment of  $\mathbf{n}$  is perpendicular to it.

### 3 Numerical scheme

The numerical scheme is a linearly implicit discretization, as the one considered in [1] and [7], in which the implicit part is discretized using a second-order backward difference formula (BDF) and the explicit part corresponds to a second order Adams-Bashforth method. The scheme can be written as

$$\frac{\frac{3}{2}\phi_1^{n+1} - 2\phi_1^n + \frac{1}{2}\phi_1^{n-1}}{\Delta t} = \gamma\lambda\nabla^2\phi_2^{n+1} + 2\mathcal{F}(\phi_1^n, \phi_2^n, \mathbf{n}^n) - \mathcal{F}(\phi_1^{n-1}, \phi_2^{n-1}, \mathbf{n}^{n-1}), \quad (6)$$

$$\phi_2^{n+1} = \frac{\alpha}{\varepsilon^2}\phi_1^{n+1} - \nabla^2\phi_1^{n+1}, \quad (7)$$

$$\frac{\frac{3}{2}\mathbf{n}^{n+1} - 2\mathbf{n}^n + \frac{1}{2}\mathbf{n}^{n-1}}{\Delta t} = \tau K\beta\nabla^2\mathbf{n}^{n+1} + 2\mathcal{G}(\phi_1^n, \mathbf{n}^n) - \mathcal{G}(\phi_1^{n-1}, \mathbf{n}^{n-1}), \quad (8)$$

where

$$\begin{aligned} \mathcal{F}(\phi_1, \phi_2, \mathbf{n}) = & \gamma\nabla^2 \left[ \frac{\lambda}{\varepsilon^2} (\phi_1^3 - \phi_1) + \frac{K}{4} \left( \nabla\mathbf{n} : (\nabla\mathbf{n})^T + \frac{(|\mathbf{n}|^2 - 1)^2}{2\delta^2} \right) + \right. \\ & \left. + \mu_{\text{anch}} \right] - \gamma\lambda\frac{\alpha}{\varepsilon^2} \left( \frac{\alpha}{\varepsilon^2}\phi_1 - \phi_2 \right), \end{aligned} \quad (9)$$

$$\begin{aligned} \mathcal{G}(\phi_1, \mathbf{n}) = & \tau K \left[ \nabla \cdot \left( \frac{1 + \phi_1}{2} \nabla\mathbf{n} \right) - \frac{1 + \phi_1}{2} \frac{(|\mathbf{n}|^2 - 1)\mathbf{n}}{\delta^2} \right] - \tau\mathbf{g} + \\ & - \tau K\beta\nabla^2\mathbf{n}, \end{aligned} \quad (10)$$

and  $\mu_{\text{anch}}$  is given by

$$\mu_{\text{anch}} = \begin{cases} -A\nabla \cdot [(\mathbf{n} \cdot \nabla\phi_1)\mathbf{n}] & \text{(planar anchoring),} \\ -A\nabla \cdot [|\mathbf{n}|^2\nabla\phi_1 - (\mathbf{n} \cdot \nabla\phi_1)\mathbf{n}] & \text{(homeotropic anchoring),} \end{cases} \quad (11)$$

and  $\mathbf{g}$  by

$$\mathbf{g} = \begin{cases} A(\mathbf{n} \cdot \nabla\phi_1)\nabla\phi_1 & \text{(planar anchoring),} \\ A [ |\nabla\phi_1|^2\mathbf{n} - (\mathbf{n} \cdot \nabla\phi_1)\nabla\phi_1 ] & \text{(homeotropic anchoring).} \end{cases} \quad (12)$$

In the simulations reported in this work we take  $\alpha = 2$  and  $\beta = 1$ . In addition, to limit the terms  $(1 + \phi)/2$  from exceeding 1 due to numerical overshoot, we approximate this term by  $(1 + s\phi)/2$ , where  $s = 0.90$ . Equations (6)-(12) are solved on a cube  $[0, 2] \times [0, 2] \times [0, 2]$  with periodic boundary conditions. The spatial derivatives are discretized with standard second order finite differences on a uniform grid  $256 \times 256 \times 256$  and linear systems arising from the discretization are solved through the multigrid [6] [7] [14] [15]. The time step  $\Delta t$  used is equal to  $10^{-1}$  and spatial step  $h = \Delta x = \Delta y = \Delta z$  is equal to  $\frac{2}{256}$ .

### 4 Results

Following [11] and [19], we take  $\lambda = 1.342 \times 10^{-2}$ ,  $\gamma = 4 \times 10^{-5}$ ,  $\delta = 6.25 \times 10^{-2}$ , and  $A = 6.708 \times 10^{-3}$ . To balance anchoring and elastic energy we select  $K = A$ . The relaxation time  $\tau$  is taken to be 1 and  $\varepsilon = \frac{4}{256}$ .

To simulate spinodal decomposition with planar and homeotropic anchoring, we consider initial condition starting from the slightly, randomly perturbed homogenous phase  $\phi \equiv 0$ . To this end, we take the initial order parameter  $\phi_0$  at each grid point  $(x_i, y_j, z_k)$  to be  $\phi_0(x_i, y_j, z_k) = 0.0 + \xi_{ijk}$ , where  $\xi_{ijk}$  is a uniformly distributed random number in  $(-\varepsilon, \varepsilon)$ . The parameter  $\varepsilon$  is the same as that in the mixing energy, i.e., a measure of the interfacial thickness. The initial director field  $\mathbf{n}_0$  is given by  $\mathbf{n}_0(x_i, y_j, z_k) = \frac{(1, 1, \omega_{ijk})}{\sqrt{2 + \omega_{ijk}^2}}$ ,  $\omega_{ijk} \in (-0.05, 0.05)$ . Figures 1 and 2 show the director vector field of the spinodal decomposition with planar and homeotropic anchoring, respectively. In both cases, it is possible to verify that the phase separation occurs very slowly and there is the formation of a coarsening pattern with a bicontinuous structure. The morphology and the coarsening dynamics are both dramatically affected by the orientational distortions of the director field. The nematic phase and the anchoring conditions largely control the morphology and slow down the ordering kinetics. This can be proved comparing the simulations with planar and homeotropic anchoring with simulations without anchoring, as those present in [1] [7] [14] [15]. Figure 3 shows phase separation at later times. The initial islands merge in horizontal lamellae in planar case (Figure 3(a)) and vertical lamellae in homeotropic case (Figure 3(b)). These results are consistent with the 2D results found by Mata et al [11].

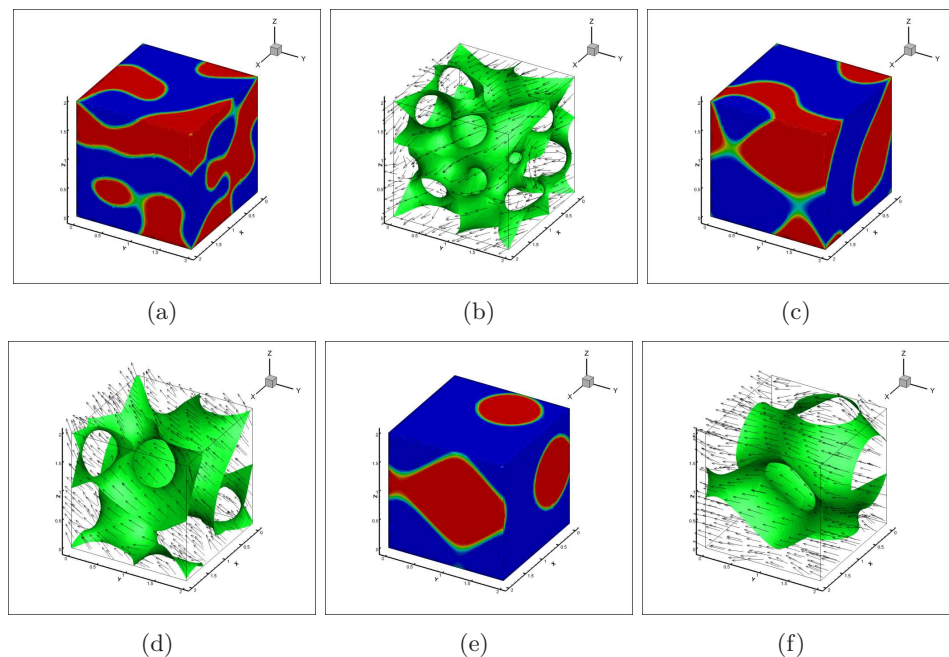


Figure 1: Spinodal decomposition with planar anchoring: contour and isosurfaces ( $\phi = 0$ ) with director field at  $t = 2050$  ((a)-(b)),  $t = 13800$  ((c)-(d)) and  $t = 24000$  ((e)-(f)).

To simulate spinodal decomposition with nucleation, we take the initial condition  $\phi_0(x_i, y_j, z_k) = 0.5 + \xi_{ijk}$ , where  $\xi_{ijk} \in (-\varepsilon, \varepsilon)$ . This corresponds to a small random perturbation of the homogeneous state  $\phi \equiv 0.5$  where the liquid crystal is the dominant component. The initial director field is selected as in planar and homeotropic cases. Fi-

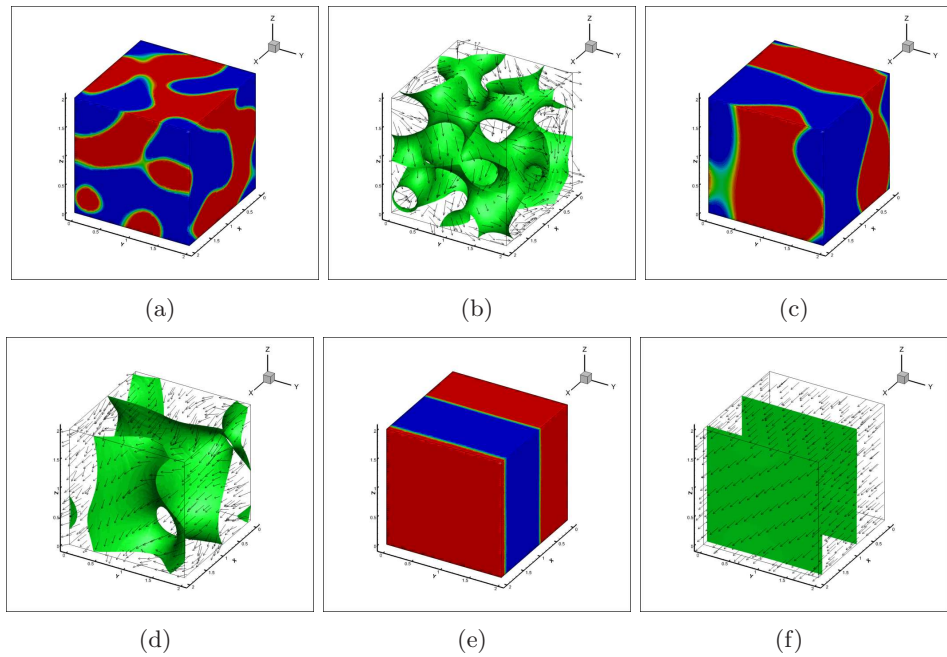


Figure 2: Spinodal decomposition with homeotropic anchoring: contour and isosurfaces ( $\phi = 0$ ) with director field at  $t = 2050$  ((a)-(b)),  $t = 13800$  ((c)-(d)) and  $t = 23000$  ((e)-(f)).

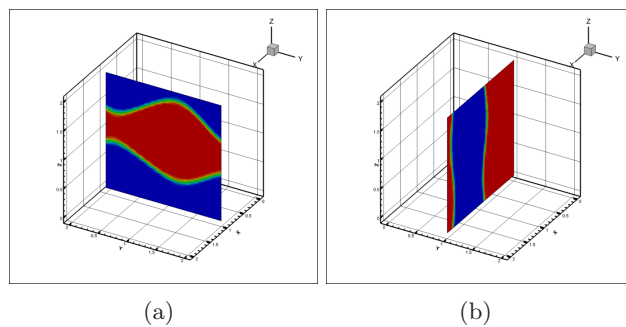


Figure 3: (a) Spinodal decomposition with planar anchoring: contour at  $x = 1$  and  $t = 18000$ ; (b) spinodal decomposition with homeotropic anchoring: contour at  $y = 1$  and  $t = 18000$ .

Figure 4 shows spinodal decomposition with nucleation and homeotropic anchoring. It can be observed that the numerous drops defined by the initial condition coalesce forming a single large drop.

## 5 Conclusions

We simulated, using Model B, three-dimensional spinodal decomposition of a two-phase mixture where the components are a nematic liquid crystal and a flexible polymer.

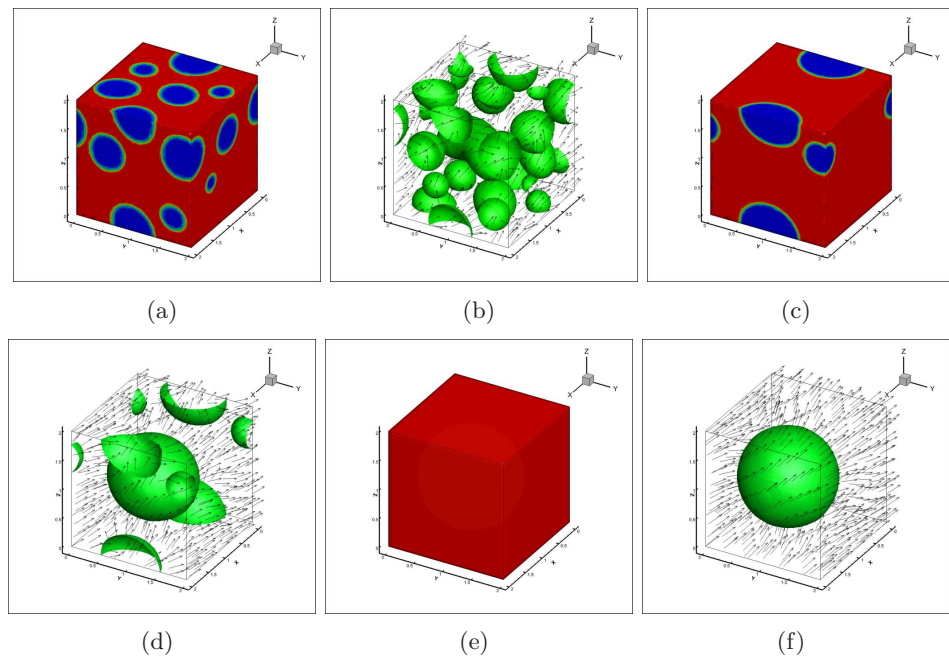


Figure 4: Spinodal decomposition with nucleation and homeotropic anchoring: contour and isosurfaces ( $\phi = 0$ ) with director field at  $t = 900$  ((a)-(b)),  $t = 5050$  ((c)-(d)) and  $t = 18000$  ((e)-(f)).

In the results of the simulations we can observe how the morphology of the separation is affected by the director field. These results are consistent with the two-dimensional results obtained by Mata et al [11].

## References

- [1] V. E. Badalassi, H. D. Ceniceros, and S. Banerjee, Computation of multiphase systems with phase field models, *J. Comput. Phys.*, 190:371-397, 2003.
- [2] A. J. Bray, Theory of phase-ordering kinetics, *Advances in Physics*, 43(3):357-459, 1994.
- [3] A. J. Bray, Coarsening dynamics of phase-separating systems, *Phil. Trans. R. Soc. Lond. A*, 361:781-792, 2004.
- [4] S. Bronnikov, C. Racles, and V. Cozan, Kinetics of the nematic phase growth across the isotropic-nematic phase transition in polymer-dispersed liquid crystals, *Liquid Crystals*, 36(3):319-328, 2009.
- [5] S. Bronnikov, S. Kostromin, and V. V. Zuev, Thermally induced isotropic-nematic phase separation in mixtures of low-molecular weight and polymer liquid crystals, *Soft Materials*, 11(1):6-12, 2013.

- [6] H. D. Cenicerros, and A. M. Roma, A nonstiff, adaptive, mesh refinement-based method for the Cahn-Hilliard equation, *J. Comput. Phys.*, 225(2):1849-1862, 2007.
- [7] H. D. Cenicerros, R. L. Nos, and A. M. Roma, Three-dimensional, fully adaptive simulations of phase-field fluid models, *J. Comput. Phys.*, 229(17):6135-6155, 2010.
- [8] P. G. de Gennes, and J. Prost. *The physics of liquid crystals*. Clarendon Press, 1993.
- [9] P. C. Hohenberg, and B. I. Halperin, Theory of dynamic critical phenomena, *Rev. Mod. Phys.*, 49(3):435, 1977.
- [10] Y. J. Jeon, Y. Bingzhu, J. T. Rhee, D. L. Cheung, and M. Jamil, Application and new developments in polymer-dispersed liquid crystal simulation studies, *Macromolecular Theory and Simulations*, 16(7):643-659, 2007.
- [11] M. Mata, C. J. García-Cervera, and H. D. Cenicerros, Ordering kinetics of a conserved binary mixture with a nematic liquid crystal component, *Journal of Non-Newtonian Fluid Mechanics*, 212:18-27, 2014.
- [12] A. Matsuyama, and R. Hirashima, Phase separations in liquid crystal-colloid mixtures, *The Journal of Chemical Physics*, 128(4), 2008.
- [13] M. Motoyama, H. Nakazawa, T. Ohta, T. Fujisawa, H. Nakada, M. Hayashi, and M. Aizawa, Phase separation of liquid crystal-polymer mixtures, *Computational and Theoretical Polymer Science*, 10(3-4):287-297, 2000.
- [14] R. L. Nos. *Simulações de escoamentos tridimensionais bifásicos empregando métodos adaptativos e modelos de campo de fase*. Tese de Doutorado, IME/USP, 2007.
- [15] R. L. Nos, H. D. Cenicerros, and A. M. Roma, Simulação tridimensional adaptativa da separação das fases de uma mistura bifásica usando a Equação de Cahn-Hilliard, *TEMA - Trends in Applied and Computational Mathematics*, 13(1):37-50, 2012.
- [16] R. L. Nos, H. D. Cenicerros, and A. M. Roma. Three-dimensional simulations of a conserved binary mixture with a nematic liquid crystal and flexible polymer components. In *IV Simpósio de Métodos Numéricos Computacionais da Universidade Federal do Paraná*, 63-69, 2014.
- [17] R. L. Nos, H. D. Cenicerros, and A. M. Roma. Three-dimensional simulations of a conserved binary mixture using Model B. In *Proceedings of Congress on Numerical Methods in Engineering*, Lisboa, 2015.
- [18] J. Xia, J. Wang, Z. Lin, F. Qiu, and Y. Yang, Phase separation kinetics of polymer dispersed liquid crystals confined between two parallel walls, *Macromolecules*, 39(6):2247-2253, 2006.
- [19] P. Yue, J. J. Feng, C. Liu, and J. Shen, A diffuse-interface method for simulating two-phase flows of complex fluids, *J. Fluid Mech.*, 515:293-317, 2004.